



Original Article

Biodistribution, pharmacokinetics and toxicity of a *Vasconcellea cundinamarcensis* proteinase fraction with pharmacological activityFernanda O. Lemos^a, Maria Imaculada C. Villalba^a, Carlos A. Tagliati^c, Valbert N. Cardoso^c, Carlos E. Salas^{b,*}, Miriam T.P. Lopes^a^a Departamento de Farmacologia, Instituto de Ciências Biológicas, Universidade Federal de Minas Gerais, Belo Horizonte, MG, Brazil^b Departamento de Bioquímica e Imunologia, Instituto de Ciências Biológicas, Universidade Federal de Minas Gerais, Belo Horizonte, MG, Brazil^c Departamento de Análises Clínicas e Toxicológicas, Faculdade de Farmácia, Universidade Federal de Minas Gerais, Belo Horizonte, MG, Brazil

ARTICLE INFO

Article history:

Received 9 June 2015

Accepted 29 September 2015

Available online 10 November 2015

Keywords:

Caricaceae

Cysteine proteinases

Biodistribution

Pharmacokinetics

Toxicity

ABSTRACT

Prior studies demonstrate that a proteinase fraction from *Vasconcellea cundinamarcensis* V.M. Badillo, Caricaceae, exhibits wound healing activity in gastric and cutaneous models and antitumoral/antimetastatic effects. Here, we present the toxicity, pharmacokinetics and biodistribution data for this proteinase fraction following a single dose into Swiss mice by *i.v.*, *s.c.* or *p.o.* routes. The *i.v.* and *s.c.* toxicity assays demonstrate that proteinase fraction at ≤ 20 mg/kg is non-lethal after single injection, while parental administration (*p.o.*) of ≤ 300 mg/kg does not cause death. Based on *p.o.* acute toxicity dose using Organization for Economic Cooperation and Development protocols, proteinase fraction ranks as Class IV “harmful” substance. Proteinase fraction shows high uptake determined as K_p (distribution tissue/blood) in organs linked to metabolism and excretion. Also, high bioavailability ($\approx 100\%$) was observed by *s.c.* administration. The blood contents following *i.v.* dose fits into a pharmacokinetic bi-compartmental model, consisting of high removal constants $-k_{el}$ 0.22 h^{-1} and k_d 2.32 h^{-1} and a half-life $-t_{1/2} = 3.13\text{ h}$. The Ames test of proteinase fraction (0.01–1%) demonstrates absence of mutagenic activity. Likewise, genotoxic evaluation of proteinase fraction (5 or 10 mg/kg, *i.p.*) shows no influence in micronuclei frequency. In conclusion, the acute doses for proteinase fraction lack mutagenic and genotoxic activity, clearing the way for clinical assays.

© 2015 Sociedade Brasileira de Farmacognosia. Published by Elsevier Editora Ltda. All rights reserved.

Introduction

The study of plant cysteine proteinases attracts interest because of their multiple alleged activities. The pharmacological action described for these proteins include anthelmintic action against nematode infection (Gomes et al., 2011), anti-inflammatory activity (Gaspani et al., 2002; Brien et al., 2004) wound debridant (Ford et al., 2002; Ayello and Cuddigan, 2004; Melano et al., 2004) and to antagonize animal morbidity due to septic shock (Lima-Filho et al., 2010). The antitumoral/antimetastatic activity is perhaps one of the most attractive properties of plant cysteine proteinases, as this effect was demonstrated in enzymes from different sources (Beuth, 2008; Wald, 2008).

Cysteine proteinases from *Vasconcellea cundinamarcensis* V.M. Badillo latex have been characterized biochemically (Teixeira et al., 2008) and pharmacologically by our research group. The species is member of the Caricaceae family common to many areas in

South America. Until now, studies using P1G10, a proteinase fraction obtained by gel filtration on Sephadex G-10, shows interesting pharmacological activities, such as; wound healing of dermabrasions (Lemos et al., 2011), burns (Gomes et al., 2010), gastric ulcer protective and healing effects by *p.o.* route (Mello et al., 2006, 2008; Araujo e Silva et al., 2015). Besides, mitogenic, angiogenic and anti-inflammatory effects are evident along with the healing effect. Subcutaneous administration of P1G10 exhibits antitumor/antimetastatic activity. Apoptosis, inhibition of angiogenesis and a loss of cell adhesion to extracellular components are associated to the antitumoral effect (Dittz et al., 2010, 2015). In addition, *s.c.* proteolytically active P1G10 acts as antithrombotic (Bilheiro et al., 2013) and this effect is accompanied by a decline in platelet activation, increase in prothrombin (PT), thrombin (TT) and activated partial thromboplastin times (APTT), along with fibrinolytic and fibrinolytic action.

Previous *in vivo* studies (Lemos et al., 2011) demonstrate that P1G10 at concentrations 10-fold higher than the effective dose (0.1%, w/w in Polawax[®]) does not induce apparent changes on intact skin. Also, continuous topical application of P1G10 0.1%

* Corresponding author.

E-mail: cesbufmg@icb.ufmg.br (C.E. Salas).

during 6-month did not induce skin damage as demonstrated by microscopic examination. Also, chronically (6-month) treated specimens showed no changes in weight or histology of organs. The absence of systemic effect was anticipated considering the small amount of active principle in Polawax® that permeates intact or scarified skin (<0.3% and 26% relative to the total amount applied, respectively) (Lemos et al., 2011).

In this study, we synthesize ^{99m}Tc -P1G10 to evaluate the pharmacokinetics parameters following a single injection, and study the toxicological and mutagenic effects aiming studies at prospective therapeutic use of the formulated product.

Material and methods

Materials

Unripe fruits of *Vasconcellea cundinamarcensis* V.M. Badillo, Caricaceae, 2–4 year-old, were the source of latex used in this study. A voucher specimen of the plant was deposited at the herbarium of the Universidad de La Serena, Chile, with #15063. Benzoyl-D,L-arginine-*p*-nitroanilide (BAPNA) was from Sigma Co. Sephadex G-10 and G-15 were from GE Healthcare, ^{99m}Tc was produced in a $^{99}\text{Mo}/^{99m}\text{Tc}$ generator and provided by IPEN (São Paulo, Brazil) and each reagent used was analytical grade.

Animals

Swiss mice (male and female), approximately 8-weeks old, were obtained from CEBIO-ICB, UFMG animal facility and housed in polycarbonate cages with sawdust bedding and maintained in environmentally controlled rooms ($22 \pm 2^\circ\text{C}$ and $50 \pm 10\%$ relative humidity) with a 12-h light-dark cycle (light from 7 a.m. to 7 p.m.). Food and water were available ad libitum. The project was approved by the Ethics Committee on Animal Experimentation (CETEA) from UFMG (Process n°. 236/2008 and 91/2009).

Methods

Isolation and characterization of P1G10 fraction

Latex was collected by making three longitudinal incisions onto the surface of unripe fruits with the aid of a sharp steel blade. Following collection into a plastic dark container, it was stored at -20°C until lyophilized. Dried latex was dissolved and incubated at room temperature in buffer containing 25 mM L-cysteine, 5 mM DTT, 10 mM EDTA pH 5.0 in 1 M sodium acetate solution. The suspension was centrifuged at $4000 \times g$ 10 min at room temperature and the filtered supernatant (Whatman #1) applied onto a Sephadex G-10 (25 mm \times 400 mm) previously equilibrated with 1 M sodium acetate pH 5.0. The first A_{280} nm protein absorbing fraction containing the bulk proteolytic activity, designated as P1G10 was concentrated by ultrafiltration (10,000 Da pore size) and washed three times with an equivalent volume of distilled water, lyophilized and stored at -20°C until used. The recovered yellowish powder was analyzed for its proteolytic and amidase activities, electrophoretic mobility by SDS-PAGE and the HPLC retention time, as described by Mello et al. (2008).

Protein radiolabeling

P1G10 (1 mg) was labeled with 37 MBq $\text{Na}^{99m}\text{TcO}_4$, 3.7 mM SnCl_2 and 2.6 mM NaBH_4 in a total volume of 200 μl and incubated for 20 min at room temperature as described elsewhere by Nunan et al. (2002). The labeling efficiency was assessed by the method adapted from the United States Pharmacopeia (USP 24, 2000). An aliquot of the reaction mix (2 μl) was initially chromatographed on ascending Silica gel 60 chromatography (TLC Merck) followed by Whatman #1 descending paper chromatography to monitor labeling efficacy. During the first TLC step 5 μl of the reaction mix

were spotted onto a silica plate and after sample drying the chromatogram was developed with acetone. The strip was scrapped off and 1 cm^2 fractions placed in vials and counted in an Automatic Scintillator (ANSR-Abbot, USA). Under this condition, the reduced technetium plus the radiolabeled protein remain at the application site while oxidized Tc ($^{99m}\text{TcO}_4^-$) migrated with the front of the solvent allowing assessment of the percentage of $^{99m}\text{TcO}_4$. For descending chromatography 5 μl of reaction mix were applied onto a Whatman paper strip (15 cm \times 36 cm) previously saturated with 1% BSA solution. Saline solution (0.9%) was used to develop the chromatogram. Again, the strip of paper was cut into fractions and each fraction placed into vials and the radioactivity measured in an Automatic Scintillator, as before. Under these conditions $^{99m}\text{TcO}_4^-$ and ^{99m}Tc -P1G10 migrate with the solvent front, while $^{99m}\text{TcO}_2$ remain at the origin. The percent $^{99m}\text{TcO}_2$ is determined by the distribution of radioactivity on the paper strip. The labeling yield was calculated as follows:

Labeling yield (%)

$$= \frac{\text{cpm}^{99m}\text{Tc-P1G10}}{\text{Total cpm}(\text{}^{99m}\text{Tc-P1G10} + \text{}^{99m}\text{TcO}_4 + \text{}^{99m}\text{TcO}_2)}$$

The proportion of labeled protein relative to free $^{99m}\text{TcO}_2$ was established after running parallel Sephadex G-15 (4.0 cm \times 1.5 cm) chromatographies of the labeled protein (P1G10) and a control containing only the tracer equilibrated with 0.9% (w/v) NaCl (Nunan et al., 2002). Radioactive fractions of P1G10 were subsequently pooled and used in experiments within the next 24 h following protein labeling.

Pharmacokinetics and tissue distribution of ^{99m}Tc -P1G10

Swiss male mice (25–30 g, 8–10 weeks, $n = 48$) received 1 mg/kg ^{99m}Tc -P1G10 (0.1 ml/30 g body weight) intravenously (*i.v.*), subcutaneously (*s.c.*) or orally (*p.o.*). The animals were sacrificed by exsanguination at different intervals (0.25, 0.5, 1, 2, 4, 8, 12 and 24 h), under anesthesia with a xilazine (9 mg/kg) ketamine (60 mg/kg) mixture. Blood and urine were collected and spleen, bladder, brain, heart, stomach, liver, small- and large intestine, skin, lung, kidney, adipose tissue and thyroid were removed and weighed. The radioactivity in organs and blood was measured with an automatic scintillation counter (ANSR-Abbot, USA). The results were expressed as percentage of the injected dose per g of tissue or ml of blood. The correction for the radioisotope decay was done by simultaneous counting at a specific interval of the residual tracer equivalent to the initially injected dose. The resulting values were plotted using *Graph Pad Prism 5* software for determination of radioactivity versus time and their respective areas under the curve (AUC) and the rate constants k_{el} and k_d by a nonlinear regression model. Using the elimination constant $-k_{el}$ (slow rate slope), we calculated the half-life time ($t_{1/2}$) = $0.693/k_{el}$. The values for bioavailability (F) during *p.o.* and *s.c.* treatments were calculated by the equation:

$$F = \frac{[\text{AUC (s.c. or p.o.)} \times \text{Dose (i.v.)} \times 100]}{[\text{AUC (i.v.)} \times \text{Dose (s.c. or p.o.)}]}$$

The partition coefficient of tissue versus blood (K_p) was determined by the ratio; $\text{AUC}_{\text{organ}}/\text{AUC}_{\text{blood}}$ as before by Gibaldi and Perrier (1982).

Acute oral toxicity test

Swiss female mice were allowed to adapt for 7 days before treatment. After this period, P1G10 (5, 10, 20 or 300 mg/kg) or the vehicle (0.9% NaCl-saline) were administrated intravenously (*i.v.*), subcutaneously (*s.c.*) or by gavage (*p.o.*) at a single dose. Mice survival and clinical signs were scored (abdominal contraction, tremors,

hair coat, convulsions, paralysis, muscle tone, behavior – restlessness, apathy and isolation, or others), following [OECD 420 guideline \(2001\)](#). After 14-days observation, mice were sacrificed and the organs macroscopically examined and weighed. All clinical signs were recorded and classified according to the intensity of the effects as follows: absent (–), present or slightly (+), moderately (++), and strongly increased (+++).

Mutagenicity test

P1G10 was assayed for its mutagenic activity using the *Salmonella typhimurium* (strains TA97, TA98, TA100 and TA102) procedure with and without S9 activation ([Maron and Ames,](#)

[1983](#)). Bacterial stocks (10 μ l) were initially incubated in nutrient medium for 12–18 h at 37 °C with shaking followed by inoculation in agar/histidine/biotin plates and incubated at 37 °C for 48 h, as described by [Mortelmans and Zeiger \(2000\)](#). The bacterial cultures (100 μ l) grown from isolated colonies were added to 500 μ l of S9 or phosphate buffer (-S9) and 200 μ l of positive control, negative control (deionized water) or P1G10 (0.1, 1 or 10 mg/ml) and 500 μ l of agar containing biotin–histidine (0.5 mM) and incubated at 37 °C for 48 h. Sodium azide (5 μ g/plate, TA100), 4-nitro-*o*-phenylenediamine (2.5 μ g/plate, TA98), 9-aminoacridine (50 μ g/plate TA97), and mitomycin C (5 μ g/plate, TA102) were used as positive controls without enzymatic induction while 2-aminoanthracene (5 μ g/plate) was used with each strain, in the

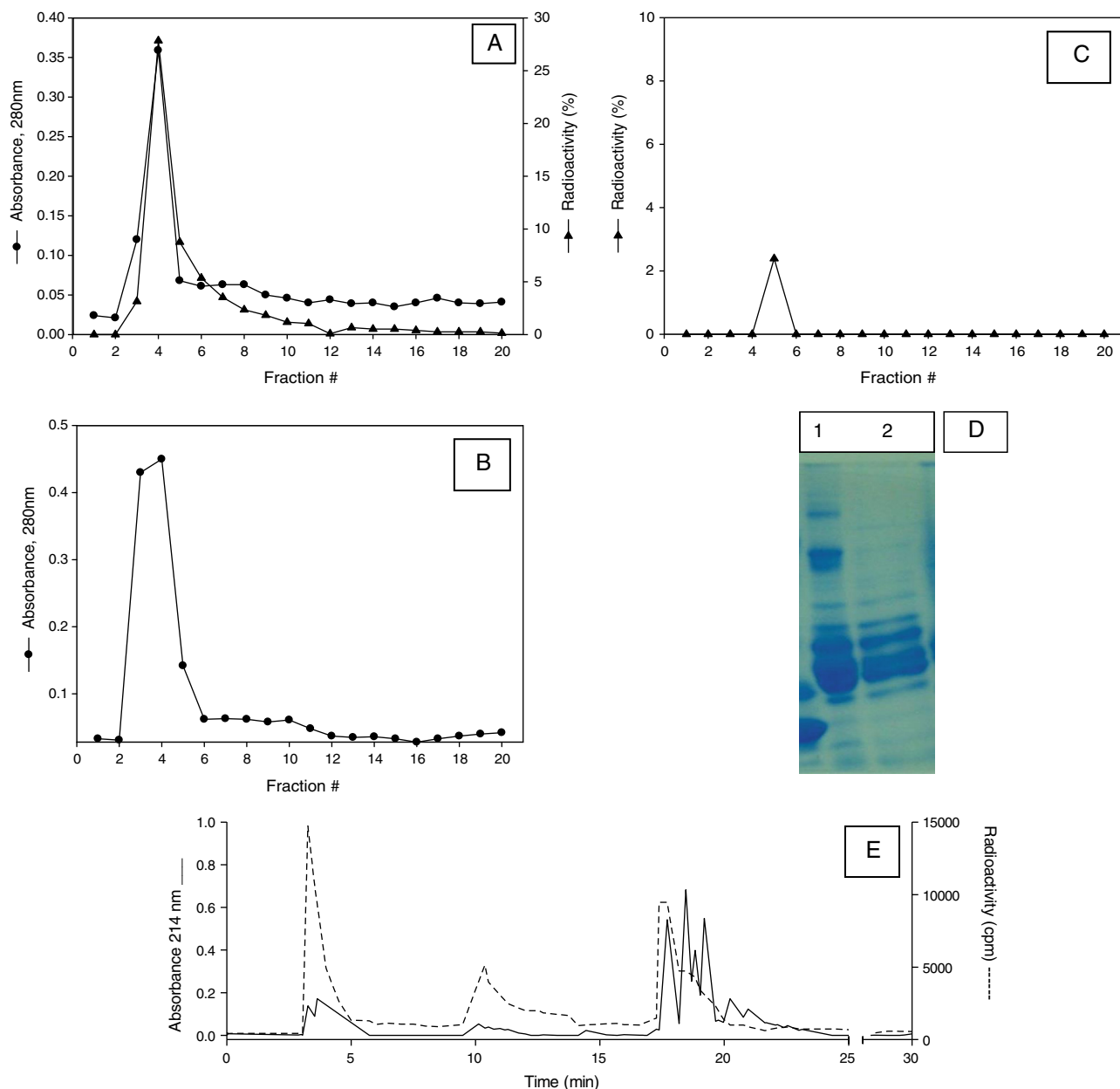


Fig. 1. Chromatographic purification and characterization of radiolabeled ^{99m}Tc P1G10. (A) ^{99m}Tc -P1G10, (B) P1G10 and (C) $^{99m}\text{TcO}_4^- + ^{99m}\text{TcO}_2$ after filtration in Sephadex G-15 column. Two hundred microliters of P1G10 (5 $\mu\text{g}/\mu\text{l}$) or ^{99m}Tc -P1G10 (5 $\mu\text{g}/\mu\text{l}$ – 1 mCi), or $^{99m}\text{TcO}_4^- + ^{99m}\text{TcO}_2$ (3.7 MBq) were applied onto Sephadex G-15 column. Fractions (0.7 ml) were collected at flow rate 0.7 ml/min. The protein profile was determined at 280 nm and the radioactivity assessed in a dose calibrator Capintec. (D) SDS-PAGE electrophoresis of P1G10 and ^{99m}Tc -P1G10. Heat-denatured protein samples (30 μg) were loaded onto each lane. Lane 1; P1G10. Lane 2 ^{99m}Tc -P1G10. (E) HPLC reverse-phase chromatography of ^{99m}Tc -P1G10. The C4 column (Vydac) was equilibrated with 0% acetonitrile – 0.1% TFA before injection of P1G10 dissolved in milli-Q water followed by elution with a non-linear acetonitrile – 0.1% TFA gradient at a flow rate of 1 ml/min (0–54% acetonitrile for 20 min; 54–81% acetonitrile for 10 min; 81–90% acetonitrile for 10 min).

presence of S9 microsomal fraction. The samples were assayed in triplicate and the results expressed as the number of colony revertant colonies per plate (Maron and Ames, 1983; Mortelmans and Zeiger, 2000). Statistical analysis was performed by ANOVA followed by Bonferroni post-test ($p < 0.05$). Mutagenicity ratio (MR) was expressed as the ratio between the number of revertant colonies for the sample and the negative control.

Micronucleus test

Male Swiss mice were treated with vehicle (castor oil) – negative control, cyclophosphamide (50 mg/kg) – positive control or P1G10 (5 mg/kg or 10 mg/kg), *i.p.*, in a single dose ($n = 5$). After 36 h interval, the animals were sacrificed by cervical dislocation and the bone marrow immediately flushed out from femora and tibia using 3 ml of fetal bovine serum and centrifuged at $1200 \times g$, 1 min. The pellet was suspended in 0.5 ml fetal bovine serum and smears were prepared on microscope slides, air dried and stained with May Grunwald. The frequency of polychromatic erythrocyte (PCE) micronucleated (at least 1 micronucleus) was determined after scoring 2000 PCE by slide (3/animal). Statistical analyzes were performed by ANOVA test followed by Bonferroni post-test ($p < 0.05$).

Results

P1G10 represents the bulk of proteolytic activity recovered from latex after Sephadex-G10 filtration as described earlier by Mello et al. (2008). To verify the uniformity of P1G10, several P1G10 batches from different latex stocks were analyzed confirming identical electrophoretic profiles on 12% SDS-PAGE (Supplementary Fig. 1A). The two higher size bands in Supplementary Fig. 1A, lines 1–5 (58 kDa and 90 kDa) represent protein aggregates, formed during lyophilization (observe that total latex sample lacks these bands, lanes 6–8). We further confirm the presence of four major protein peaks following C4-reverse phase HPLC chromatography (Supplementary Fig. 1B). The resulting protein concentration and amidase activity of P1G10 were 8.39 ± 0.39 mg/ml and 13.5 ± 0.5 nM/ $\mu\text{g} \times \text{min}$, respectively; this fraction was further used in toxicological and pharmacokinetics experiments described below.

Biodistribution and pharmacokinetics

Under this labeling condition $74.5 \pm 6.4\%$ ($n = 6$) yield of radiolabeled protein was recovered when reacting 1 mg P1G10 with 37 MBq $\text{Na}^{99\text{m}}\text{TcO}_4$, 3.7 mM SnCl_2 and 2.6 nM NaBH_4 , plus a small amount of TcO_4^- (0.1–1.0%) and 20–30% of TcO_2 , as confirmed by descending and ascending chromatographies (not shown). Fig. 1A illustrates the elution profile of the radiolabeled protein, following Sephadex G-15 chromatography. It shows a coincident radioactive and protein profile; the pooled fractions (3–5) representing 40–50% of the applied radioactivity and 92% of the loaded protein, as assessed by absorption at UV₂₈₀ nm. Two control chromatographies are included in Fig. 1B and C. The first one shows the protein profile (A_{280} nm) corresponding to P1G10 incubated without the radioactive, and the second one, the elution profile of TcO_2 after incubation with other ingredients but without the protein. Both radioactive peaks elute in similar fractions (compare Fig. 1A and 1C), indicating that the radioactivity in Fig. 1A is mostly due to $^{99\text{m}}\text{Tc}$ -P1G10. The assumption is also based on the amount of radioactivity recovered in fraction 5 (Fig. 1C) that represents less than 3% of the total amount loaded in the column (37 mBq). It suggests that the unreacted radioactivity is held in the column after extensive washing, while the radioactivity recovered in the protein peak (Fig. 1A) approaches 50% of the amount applied.

Table 1
Partition coefficient of $^{99\text{m}}\text{Tc}$ -P1G10 in mice organs.

Organ	Administration routes					
	<i>i.v.</i>		<i>s.c.</i>		<i>p.o.</i>	
	AUC	Kp	AUC	Kp	AUC	Kp
Blood	10.9	1.0	12.1	1.0	0.9	1.0
Liver	45.2	4.1	19.2	1.6	2.1	2.3
Spleen	12.7	1.2	6.5	0.5	0.7	0.8
Stomach	7.9	0.7	5.3	0.4	292.2	323.9
Small intestine	12.3	1.1	11.9	1.0	55.0	61.0
Large intestine	57.2	5.2	30.9	2.6	400.6	444.1
Kidney	504.9	46.3	490.9	40.7	5.6	6.2
Bladder/urine	1192.0	109.3	1263.0	104.6	29.4	32.6
Thyroid	5.7	0.5	8.3	0.7	1.5	1.6
Fat	3.5	0.3	3.1	0.3	0.3	0.4
Brain	0.6	0.1	1	0.1	0.1	0.1
Heart	6.9	0.6	6.7	0.6	0.6	0.7
Lung	10.7	1.0	8.7	0.7	0.7	0.8
Skin	7.8	0.7	7.5	0.6	1.6	1.8

AUC, area under the curve; Kp, partition coefficient; Administration routes: *i.v.*, intravenous; *s.c.*, subcutaneous; *p.o.*, oral. Dose: 1 mg/kg $^{99\text{m}}\text{Tc}$ -P1G10. Radioactive dose = 3 mBq.

The electrophoretic and HPLC profiles of $^{99\text{m}}\text{Tc}$ -P1G10 were evaluated to verify the existence of possible changes in mobility or retention due to radiolabeling. The protein profile depicting species with $M_w \approx 25$ kDa is similar in both, the P1G10 and the $^{99\text{m}}\text{Tc}$ -P1G10 fractions (Fig. 1D). Also, the HPLC profile and the retention time of $^{99\text{m}}\text{Tc}$ -P1G10 (Fig. 1E) using a C4 hydrophobic chromatography was similar to the P1G10 (Supplementary Fig. 1B). Besides, the overlap of radioactive and absorbance peaks indicate that the bulk of the protein is radiolabeled (Fig. 1E). The stability of $^{99\text{m}}\text{Tc}$ -P1G10 was determined by incubation of the fraction at 37 °C during various intervals (0–24 h) of the radiolabeled protein with plasma withdrawn from Swiss mice. It was observed that the percentage of $^{99\text{m}}\text{TcO}_4^-$ plus TcO_2 present in the mix remained stable totalizing 10% of total radioactivity after the incubation period, arguing for the stability of $^{99\text{m}}\text{Tc}$ -P1G10 complex (Supplementary Table 1). In short, the experimental evidence suggests that radiolabeled P1G10 remains essentially similar to the unlabeled protein and represents the major species available following protein radiolabeling.

The $^{99\text{m}}\text{Tc}$ -P1G10 distribution expressed as partition coefficient (Kp – AUC organ/AUC blood) is shown in Table 1 and the uptake kinetics of $^{99\text{m}}\text{Tc}$ -P1G10 in different organs is presented in supplementary Fig. 2. Overall, *i.v.* or *s.c.* administration resulted in high Kps in organs linked to excretion; kidney (46.3 and 40.7), bladder (109.3 and 104.6) and lower in metabolic organs; liver (4.1 and 1.6) large intestine (5.2 and 2.6), respectively. In addition, Kps for stomach (323.9) and small intestine (444.1) became comparatively large during *p.o.* injection. On the other hand, in adipose tissue, brain

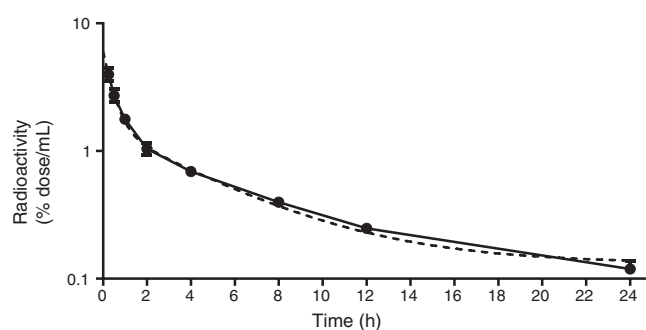


Fig. 2. Blood radioactive clearance of $^{99\text{m}}\text{Tc}$ -P1G10 injected in Swiss mice. Blood clearance of $^{99\text{m}}\text{Tc}$ -P1G10 (experimental, \blacksquare) and the nonlinear theoretical regression plot (\cdots), after *i.v.* administration. The ordinate is expressed as radioactivity (log scale) relative to the initial injected radioactivity (cpm) per ml of blood ($R^2 = 0.9998$).

Table 2
Pharmacokinetic parameters of ^{99m}Tc-P1G10 in Swiss mice.

Pharmacokinetic parameters	
k_d (h ⁻¹)	2.32 ± 1.03
k_{el} (h ⁻¹)	0.22 ± 0.20
$t_{1/2}$ distribution (h)	0.29 ± 0.67
$t_{1/2}$ elimination (h)	3.13 ± 3.42
AUC (% dose/ml × h)	10.9
Oral bioavailability (%)	8.3
Subcutaneous bioavailability (%)	111

The pharmacokinetic data for ^{99m}Tc-P1G10s was determined after a single dose of 1 mg/kg ^{99m}Tc-P1G10. Radioactive dose = 3 MBq. k_d , distribution constant; k_{el} , elimination constant; $t_{1/2}$, half-life; AUC, area under the curve.

heart, lung, thyroid and skin Kps became lower or remain close to blood levels, regardless of the administration route.

The pharmacokinetics parameters following *i.v.* administration of ^{99m}Tc-P1G10 obtained by plotting the log of percent radioactivity in blood versus time during a 24h interval, is shown in Fig. 2. The profile of radioactive decay was assimilated into a two-compartment open model composed by an initial *fast phase*, representing mainly the distribution phase (0–3 h) and the subsequent slow phase corresponding to the *disposal phase* (5–12 h). The estimated half-life of the distribution phase was 0.3 h and for the disposition phase was 3 h. A summary of the pharmacokinetics parameters is presented in Table 2.

We also compared the bioavailability of ^{99m}Tc-P1G10 following three strategies for administration. Clearly, *i.v.* and *s.c.* provide the largest availability attaining 100% in both cases, on the other hand oral administration resulted in limited bioavailability attaining less than 10% (Table 2).

Acute toxicity

In Table 3, P1G10 toxicity was shown as number of obits or the number of animals bearing clinical signs, a principal toxic event described by OECD 420 (2001). These results show absence of toxicological symptoms, both in controls and P1G10 treated animals regardless the administration route, after 14-days of treatment. The absence of toxicity was confirmed by histopathology of different organs (heart, liver, spleen, kidney, stomach, lung and large/small intestine) (data not shown). Although toxic effects at the local of injection were observed in the groups treated by *i.v.* and *s.c.* routes, remission of the signs occurred until the 14th day. Using the largest

Table 3
Systemic toxicity following a single dose of P1G10 in Swiss mice.

Route	Dose (mg/kg)	T/D	T/P	Clinical signs
<i>i.v.</i>	Control	5/0	(–)	(–)
	5	5/0	5/2	Phlebitis (+) Remission 7–12 days
	10	5/0	5/3	Phlebitis (++) Remission 7–12 days
	20	5/0	5/5	Phlebitis (+++) Remission 7–14 days
<i>s.c.</i>	Control	5/0	(–)	(–)
	5	5/0	(–)	(–)
	10	5/0	5/2	Cutaneous lesion (++) Remission in 9 days
	20	5/0	5/5	Cutaneous lesion (+++) Remission 9–14 days
<i>p.o.</i>	Control	5/0	(–)	(–)
	5	5/0	(–)	(–)
	10	5/0	(–)	(–)
	300	5/0	(–)	(–)

A single dose of P1G10 was given by *i.v.*, *s.c.* or *p.o.* route. T/D = number of treated animals/number of deaths, T/P = number of treated animals/number of positive symptoms, $n = 5$. The examination period for clinical signs after single administration was 15, 30, 60 min and every hour during 12 h and daily during 14 days. The control vehicle was 0.9% NaCl. Code for observed symptoms: (–), absent; (+), present or slightly increased; (++) , moderately increased; (+++) , strongly increased.

i.v. dose (20 mg/kg) every animal exhibited severe symptoms of phlebitis. Forty and 60% of animals that received 5 and 10 mg/kg, respectively, showed slight or moderate signs of phlebitis. During *s.c.* administration, all animals showed severe cutaneous lesions at the application site with 20 mg/kg, whereas 40% of animals that received 10 mg/kg showed light to moderate sign of lesions.

The mutagenic activity of P1G10 measured by Ames test is presented in Table 4. The different concentrations of P1G10 (0.1, 1.0 and 10.0 mg/plate) did not induce reversion above background with the four strains analyzed, both, in the absence or presence of the microsomal activation extract (S9). A reference positive control showing significantly higher reversion was included with these experiments ($p < 0.05$, ANOVA, Bonferroni post-test). Using the micronuclei test to confirm the lack of mutagenic activity, we show in Fig. 3 that P1G10 at 5 (26.48 ± 8.94) and 10 mg/kg (24.56 ± 16.73) did not induce micronucleation above the control (castor oil) 40.82 ± 16.58) and was significantly lower than the

Table 4
Mutagenic activity of P1G10 using the *Salmonella typhimurium* – Ames test.

Treatment (mg/plate)	Revertant colonies (mean ± SD)							
	TA98		TA100		TA97		TA102	
	–S9	+S9	–S9	+S9	–S9	+S9	–S9	+S9
Negative control (H ₂ O)	21.7 ± 4.1	25.0 ± 5.4	165.3 ± 27.1	155.3 ± 25.5	171.7 ± 19.4	138.3 ± 11.4	126.7 ± 15.8	133.3 ± 18.9
P1G10								
0.1 mg (MR)	31.3 ± 1.8 (1.4)	24.3 ± 3.4 (0.9)	81.3 ± 17.4 (0.5)	66.7 ± 2.9 (0.4)	134.7 ± 27.5 (0.8)	100.3 ± 3.2 (0.72)	77.0 ± 1.2 (0.6)	128.0 ± 24.7 (1.0)
1.0 mg (MR)	19.3 ± 3.4 (0.9)	23.3 ± 2.4 (0.9)	88.0 ± 17.3 (1.0)	105.3 ± 10.4 (1.6)	128.7 ± 52.9 (0.7)	64.3 ± 4.0 (0.5)	107.0 ± 1.2 (0.8)	155.0 ± 3.9 (1.2)
10 mg (MR)	15.3 ± 2.4 (0.7)	27.3 ± 0.3 (1.1)	124.0 ± 25.7 (0.7)	117.3 ± 12.6 (0.7)	94.7 ± 1.1 (0.5)	29.3 ± 2.9 (0.2)	69.7 ± 3.5 (0.5)	166.7 ± 11.1 (1.2)
Positive control (MR)	132.9 ± 32.9 [*] (6.2)	118.6 ± 22.0 (4.7)	1211.9 ± 112.6 [*] (7.3)	1561.3 ± 121.1 [*] (10.0)	861.33 ± 174.74 [*] (5.0)	278.6 ± 106.9 [*] (2.1)	1976.6 ± 159.2 [*] (15.6)	1799.6 ± 154.1 [*] (13.5)

Salmonella typhimurium strains: TA 97, TA 98, TA 100 and TA 102; +S9 or –S9, plus or minus metabolic activator, respectively. Triplicate assays contained P1G10 (0.1, 1, 10 mg/plate); negative control: 100 µl/plate (H₂O); positive control: for TA 98, 4-nitro-o-phenylenediamine (2.5 mg/plate); TA 100, sodium azide (1.25 mg/plate); TA 97, 9-aminoacridine (50 mg/plate); TA 102, mitomycin C (0.5 g/plate); with S9 – TA 97, 98, 100 and 102, 2-aminoanthracene (5 mg/plate). MR = mutagenesis rate: number of mutants relative to negative control.

^{*} $p < 0.05$ ANOVA, Bonferroni post-test.

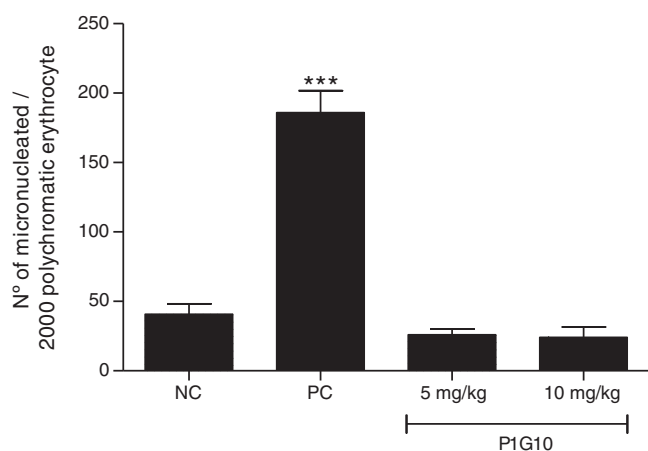


Fig. 3. The effect of P1G10 on frequency of micronucleated polychromatic erythrocytes in mice bone marrow. Erythrocyte counting (2000 polychromatic erythrocytes) was done 36 h after a single *i.p.* injection of P1G10 (5 or 10 mg/kg), cyclophosphamide 50 mg/kg or 0.9% NaCl, ($n = 5$, 3 smears/animal). The slides were stained with May Grunwald and analyzed by optical microscopy (100 \times – immersion). NC, negative control – castor oil, PC, positive control – cyclophosphamide (50 mg/kg). *** $p < 0.01$ ANOVA, Bonferroni post-test.

positive control (cyclophosphamide 50 mg/kg) 186.56 ± 35.17 ($p < 0.05$, ANOVA, Bonferroni post-test).

Discussion

Based on a biochemical characterization and pharmacological activities for cysteine proteinases (P1G10 fraction) described in latex from *V. cundinamarcensis* we analyze the pharmacokinetics, distribution and toxicology of this fraction.

Initially, the pharmacokinetics parameters were determined after *i.v.* administration of radiolabeled P1G10, while the distribution and bioavailability were also determined by *p.o.* and *s.c.* treatments. These two last routes were included as previous studies demonstrate the gastric healing and antitumor/antimetastatic activities of this fraction, respectively (Mello et al., 2008; Araujo e Silva et al., 2015; Dittz et al., 2010, 2015).

The kinetic profiles of P1G10 in blood after *s.c.* or *i.v.* administration were alike (Fig. 2), the similarity was confirmed upon determination of AUC and bioavailability following *s.c.* or *i.v.* injection (Table 2). The clearance of P1G10 or metabolites following *i.v.* administration is explained by a bi-exponential decay function (Fig. 2), appropriately described by a two compartment pharmacokinetics model (Tang et al., 2004). By applying this function we determined the pharmacokinetic parameters, listed in Table 2. The low $t_{1/2} \approx 18$ min for the distribution (fast phase) and $t_{1/2} \approx 190$ min for the elimination (slow phase) were related to rapid excretion of ^{99m}Tc -P1G10 or its metabolites. These observations are confirmed by the high initial uptake in organs related to these processes, (liver, kidneys and bladder) (Table 1). The preferential uptake of these organs was evident upon comparison of Kps for kidney or bladder/urine (Table 1) and those from lipophilic organs (brain, adipose tissue) that act as efficient barriers for hydrophilic macromolecules (Boer and Gaillard, 2007). Values similar to $t_{1/2}$ elimination for P1G10 (≈ 190 min) were reported for different proteinases. A $t_{1/2} = 150$ min elimination interval was established when ^{99m}Tc -streptokinase or ^{99m}Tc -urokinase were administered to mice and between 160–260 min in dogs given ^{131}I streptokinase (Coates et al., 1974; Som et al., 1975). In contrast the elimination $t_{1/2}$ in humans treated with bromelain attained 6.2 h (Castell et al., 1997).

The distribution analysis shows a large uptake of ^{99m}Tc -P1G10 in various organs after *i.v.* and *s.c.* relative to *p.o.* administration. As expected, the exception was the high GI presence following *p.o.*

treatment (Supplementary Fig. 2). These data suggest some type of interaction between these proteins and the GI compartment. The classical view asserts that absorption of macromolecules via *p.o.* is absent due to enzymatic degradation and/or protein denaturation influenced by gastric acidity and the presence of the mucosa barrier (Toon, 1996; Tang et al., 2004; Goldberg and Gomez-Orellana, 2003; Mahmood and Green, 2005). P1G10 may also undergo pre-systemic lymphatic clearance, contributing to the reduced uptake by different organs as described by Wasan (2002) for proteins and peptide-like drugs. On the other hand, experimental evidence suggests that a small but sizable amount of protein is absorbed through the gastrointestinal (GI) tract. Mechanisms such as; persorption, enteropancreatic circulation, receptor specific absorption, changes in transepithelial electric resistance and paracellular diffusion are invoked to explain GI protein transport (Kolac et al., 1996). In our case the absorption might be facilitated by the mucolytic action attributed to proteolytic enzymes that split amino acid bonds from mucus glycoproteins (Bock et al., 1998). Indirect evidence supporting this notion arises from several studies using proteolytic enzymes as adjuvants that facilitate the passage of non-permeable drugs (Grabovac et al., 2007). In summary, the relatively small bioavailability of P1G10 by *p.o.* (Table 2) compares well with data for protein absorption documented in mammals (Kolac et al., 1996) and exceeds the value proposed by Baumann (2006). Overall, the AUC blood value, obtained after *p.o.* route was approximately 10-fold lower than values observed after parenteral administration, resulting in less than 10% bioavailability (Table 2). Attempts to identify radiolabeled P1G10 by electrophoresis followed by autoradiography or HPLC in blood or urine were unsuccessful because of the large amount of protein contaminants in the sample and the rapid decay of radioactivity. Therefore, it is possible that the calculated 8.3% (Table 2) bioavailability represents labeled degradation products.

An interesting fact arises from analysis of the radioactive contents in stomach and large intestine after *p.o.* administration (Supplementary Fig. 2). In stomach, a strong rapid increase in radioactivity occurs lasting about 8 h and in large intestine the maximal radioactivity was seen after a 4-hour period, decreasing thereafter. By contrary, *i.v.* or *s.c.* maxima in these organs were barely detectable throughout the experiment, and the levels remained stable between 4 and 10 h. The presence of high P1G10 levels in the GI tract explains the oral effectiveness of P1G10 administration as gastroprotective or gastric healer demonstrated earlier by Mello et al. (2008) and Araujo e Silva et al. (2015).

We suggest that distribution of P1G10 in different compartments at short intervals mainly represents the intact protein since radioactive ^{99m}Tc -P1G10 showed no evidence of degradation or structural changes, following electrophoresis or HPLC analysis after synthesis (Fig. 1D and E). In addition, assays of stability with the labeled protein incubated with plasma of mice suggest that only 10% of the radioactivity represents TcO_4^- plus TcO_2 after 24 h incubation at 37 °C, thus the bulk radioactivity measured in distribution experiments corresponds to undegraded protein (Supplementary Table 1). The low proportion of byproducts was confirmed by the limited uptake into thyroid, an organ that usually incorporates radioactive impurities (Goolden et al., 1971). The literature describes a number of proteinaceous radiolabeled molecules targeted for pharmacological applications, but few of them belong to the family of proteinases (Castell et al., 1997; Kolac et al., 1996). In many of these reports the labeling efficiency approximates the yield observed in our study (Komarek et al., 2005). Thus, considering the nature of P1G10 and its physicochemical properties, such as size and hydrophilicity, we correlate these characteristics with the pharmacokinetics parameters determined with the radiolabeled fraction, and justify the rapid clearance, low *p.o.* bioavailability and minimum distribution in lipophilic organs.

The acute toxicity analysis of P1G10 via *s.c.* or *i.v.* injection showed that the fraction was not lethal below 20 mg/kg and by *p.o.* administration the animals survived at doses ≤ 300 mg/kg. Therefore, the classification for this fraction is “harmful” (category 4) when ingested (Taussig et al., 1975). Additional symptoms of toxicity were absent; this examination included: skin or fur, eyes, mucous membranes, respiratory, circulatory, autonomic, central nervous system, somatomotor activity and behavioral pattern, as established by OECD 420 (2001).

The signs of phlebitis after *i.v.* dose and the localized lesion ensuing *s.c.* injection must arise by damage to vessels due to the proteolytic activity in the sample or by interference of these enzymes in the haemostatic system, as demonstrated by Bilheiro et al. (2013). Studies with other proteinases describe bromelain as having low toxicity; the LD₅₀ in mice, rats and rabbits was >10 g/kg, and the LD₅₀ above 2 g/kg placing this enzyme below the toxic range (Taussig et al., 1975). Chronic studies in dogs showed that up to 750 mg/kg administered daily lacked toxic effects after a six-month period. In rats, a daily oral dose of 1500 mg/kg had no carcinogenic or teratogenic activity, did not impair food ingest, histology of heart, spleen, kidney or hematological parameters (Moss et al., 1963). In humans oral administration of bromelain (3000 FIP unit/day; ≈ 600 mg/day) during ten days did not alter the blood coagulation parameters. In the case of papain, the enzyme mix from *Carica papaya*, has an oral LD₅₀ of 4.000 mg/kg, and classifies in category 5 (USP 34, 2011). Thus, P1G10 has higher toxic potential compared to bromelain and papain, probably due to its high proteolytic activity, which ranks 5 to 7-fold higher than papain from *C. papaya* (Baeza et al., 1990; Teixeira et al., 2008).

The mutagenic reversion frequency of P1G10 measured by Ames reversion was similar to the background on each strain and significantly lower than the positive control. Moreover, P1G10 at the highest concentration (10 mg/plate) exhibited a MR tendency below the negative control, suggesting an antimutagenic activity (TA97 + S9, MR = 0.2, Table 4). Additional Ames experiments combining a promutagenic substances plus P1G10 must be conducted to confirm or rule out this possibility.

Similarly, the genotoxic potential of P1G10 assessed by the micronuclei assay at 5 and 10 mg/kg, showed no alteration in frequency of micronucleated polychromatic erythrocytes relative to the negative control and significantly different from the positive control cyclophosphamide at 50 mg/kg (Fig. 3, $p < 0.01$ ANOVA, Bonferroni post-test). Based on these results, it is concluded that fraction P1G10 lacks mutagenic or genotoxic activities (Pariza and Johnson, 2001).

In conclusion, the protein fraction composed by isoforms of proteolytic enzymes from *V. cundinamarcensis* shows high uptake in metabolic and excretion compartments and lower bioavailability in lipid rich compartments compatible with the hydrophilic nature of these macromolecules. The fraction does not represent a mutagenic or genotoxic hazard at doses exhibiting therapeutic effect. Based on the toxicological studies using Swiss mice the substance ranks as class IV compound, labeled as harmful.

Conflicts of interest

The authors declare no conflicts of interest.

Acknowledgments

We would like to thank Luciana M Siqueira for technical and CNPq, CAPES and FAPEMIG for financial support.

Appendix A. Supplementary data

Supplementary data associated with this article can be found, in the online version, at doi:10.1016/j.bjp.2015.09.008.

References

- Araujo e Silva, A.C., de Oliveira Lemos, F., Gomes, M.T., Salas, C.E., Lopes, M.T., 2015. Role of gastric acid inhibition, prostaglandins and endogenous-free thiol groups on the gastroprotective effect of a proteolytic fraction from *Vasconcellea cundinamarcensis* latex. *J. Pharm. Pharmacol.* 67, 133–141.
- Ayello, E.A., Cuddigan, J.E., 2004. Debridement: controlling the necrotic/cellular burden. *Adv. Skin Wound Care* 17, 66–75.
- Baeza, G., Correa, D., Salas, C.E., 1990. Proteolytic enzymes in *Carica candamarcensis*. *J. Sci. Food Agric.* 51, 1–9.
- Baumann, A., 2006. Early development of therapeutic biologics – pharmacokinetics. *Curr. Drug Metabol.* 7, 15–21.
- Beuth, J., 2008. Proteolytic enzyme therapy in evidence-based complementary oncology: fact or fiction? *Integr. Cancer Ther.* 7, 311–316.
- Bilheiro, R.P., Braga, A.D., Limborço-Filho, M., Carvalho-Tavares, J., Agero, U., Carvalho, M.G., Sanchez, E.F., Salas, C.E., Lopes, M.T.P., 2013. The thrombolytic action of a proteolytic fraction (P1G10) from *Carica candamarcensis*. *Thromb. Res.* 131, 175–182.
- Bock, U., Kolac, C., Borchard, G., Koch, K., Fuchs, R., Streichhan, P., Lehr, C.M., 1998. Transport of proteolytic enzymes across Caco-2 cell monolayers. *Pharm. Res.* 15, 1393–1400.
- Boer, A.G., Gaillard, P.J., 2007. Drug targeting to the brain. *Annu. Rev. Pharmacol. Toxicol.* 47, 323–355.
- Brien, S., Lewith, G., Walker, A., Hicks, S.M., Middleton, D., 2004. Bromelain as a treatment for osteoarthritis: a review of clinical studies. *Evid. Based Complement Alternat. Med.* 1, 251–257.
- Castell, J.V., Friedrich, G., Kuhn, C.S., Poppe, G.E., 1997. Intestinal absorption of undegraded proteins in men: presence of bromelain in plasma after oral intake. *Am. J. Physiol.* 273, G139–G146.
- Coates, G., DeNardo, S.J., DeNardo, G.L., Troy, F., 1974. Pharmacokinetics of radioiodinated streptokinase. *J. Nucl. Med.* 16, 136–142.
- Dittz, D., Figueiredo, C., Lemos, F.O., Viana, C.T., Andrade, S.P., Souza-Fagundes, E.M., Fujiwara, R.T., Salas, C.E., Lopes, M.T., 2015. Antiangiogenesis, loss of cell adhesion and apoptosis are involved in the antitumoral activity of Proteases from *V. cundinamarcensis* (*C. candamarcensis*) in murine melanoma B16F1. *Int. J. Mol. Sci.* 16, 7027–7044.
- Dittz, D., Lopes, M.T.P., Figueiredo, C., Viana, C.T.R., Salas, C.E., 2010. Antitumoral and antimetastatic activities of a proteolytic fraction from *Carica candamarcensis* latex. *Basic Clin. Pharmacol. Toxicol.* 107, 162.
- Ford, C.N., Reinhard, E.R., Yeh, D., Syrek, D., De Las Morenas, A., Bergman, S.B., Williams, S., Hamori, C.A., 2002. Interim analysis of a prospective, randomized trial of vacuum-assisted closure versus the healthpoint system in the management of pressure ulcers. *Ann. Plast. Surg.* 49, 55–61.
- Gaspari, L., Limioli, E., Ferrario, P., Bianchi, M., 2002. *In vivo* and *in vitro* effects of bromelain on PGE(2) and SP concentrations in the inflammatory exudate in rats. *Pharmacology* 65, 83–86.
- Gibaldi, M., Perrier, D., 1982. *Pharmacokinetics*. Marcel Dekker, Inc., New York.
- Goldberg, M., Gomez-Orellana, I., 2003. Challenges for the oral delivery of macromolecules. *Nat. Rev. Drug Discov.* 2, 289–295.
- Gomes, F.S., Spínola, C.V., Ribeiro, H.A., Lopes, M.T., Cassali, G.D., Salas, C.E., 2010. Wound-healing activity of a proteolytic fraction from *Carica candamarcensis* on experimentally induced burn. *Burns* 36, 277–283.
- Gomes, M.T., Oliva, M.L., Lopes, M.T.P., Salas, C.E., 2011. Plant proteinases and inhibitors: an overview of biological function and pharmacological activity. *Curr. Protein Pept. Sci.* 12, 417–436.
- Goolden, A.W., Glass, H.I., Williams, E.D., 1971. Use of ^{99m}Tc for the routine assessment of thyroid function. *Br. Med. J.* 13, 396–399.
- Grabovac, V., Schmitz, T., Föger, F., Bernkop-Schnürch, A., 2007. Papain: an effective permeation enhancer for orally administered low molecular weight heparin. *Pharm. Res.* 24, 1001–1006.
- Kolac, C., Streichhan, P., Lehr, C.M., 1996. Oral bioavailability of proteolytic enzymes. *Eur. J. Biopharm.* 42, 222–232.
- Komarek, P., Kleisner, I., Komarkova, I., Konopkova, M., 2005. Accumulation of radiolabelled low molecular peptides and proteins in experimental inflammation. *Int. J. Pharm.* 291, 119–125.
- Lemos, F.O., Ferreira, L.A., Cardoso, V.N., Cassali, G.D., Salas, C.E., Lopes, M.T., 2011. Skin-healing activity and toxicological evaluation of a proteinase fraction from *Carica candamarcensis*. *Eur. J. Dermatol.* 21, 722–730.
- Lima-Filho, J.V., Patriota, J.M., Silva, A.F., Filho, N.T., Oliveira, R.S., Alencar, N.M., Ramos, M.V., 2010. Proteins from latex of *Calotropis procera* prevent septic shock due to lethal infection by *Salmonella* enteric serovar *Typhimurium*. *J. Ethnopharmacol.* 129, 327–334.
- Mahmood, I., Green, M.D., 2005. Pharmacokinetic and pharmacodynamic considerations in the development of therapeutic proteins. *Clin. Pharmacokinet* 44, 331–347.

- Maron, D.M., Ames, B.N., 1983. Revised methods for the *Salmonella* mutagenicity test. *Mutation Res.* 113, 173–215.
- Melano, E., Rodriguez, H.L., Carrillo Jr., R., Dillon, L., 2004. The effects of Panafil when using topical negative pressure to heal an infected sternal wound. *J. Wound Care* 13, 425–426.
- Mello, V.J., Gomes, M.T., Lemos, F.O., Delfino, J.L., Andrade, S.P., Lopes, M.T., Salas, C.E., 2008. The gastric ulcer protective and healing role of cysteine proteinases from *Carica candamarcensis*. *Phytomedicine* 15, 237–244.
- Mello, V.J., Gomes, M.T.R., Rodrigues, K.C.L., Sanchez, E.F., Lopes, M.T.P., Salas, C.E., 2006. Plant proteinases: their potential as therapeutic drugs. In: Govil, J.N., Singh, V.K., Arunachalam, C. (Eds.), *Drug Development from Molecules*. Studium Press, Texas, pp. 211–224.
- Mortelmans, K., Zeiger, E., 2000. The Ames *Salmonella*/microsome mutagenicity assay. *Mutation Res.* 455, 29–60.
- Moss, I.N., Frazier, C.V., Martin, G.J., 1963. Bromelain – the pharmacology of the enzyme. *Arch. Int. Pharmacodyn* 145, 166–189.
- Nunan, E.A., Cardoso, V.N., Moraes-Santos, T., 2002. Technetium-99m labeling of tityustoxin and venom from the scorpion *Tityus serrulatus*. *Appl. Radiat. Isot.* 57, 849–852.
- OECD, 2001. *Acute Oral Toxicity: Fixed Dose Procedure – Guideline for Testing of Chemicals N. 420*. Organisation for Economic Cooperation and Development, Paris.
- Pariza, M.W., Johnson, E.A., 2001. Evaluating the safety of microbial enzyme preparations used in food processing: update for a new century. *Regul. Toxicol. Pharmacol.* 33, 173–186.
- Som, P., Rhodes, B.A., Bell, W.R., 1975. Radiolabeled streptokinase and urokinase and their comparative biodistribution. *Thromb. Res.* 6, 247–253.
- Tang, L., Persky, A.M., Hochhaus, G., Meibohm, B., 2004. Pharmacokinetic aspects of biotechnology products. *J. Pharm. Sci.* 93, 2184–2204.
- Taussig, S.J., Yokoyama, M.M., Chinenn, E.T., 1975. Bromelain: a proteolytic enzyme and its clinical application. *Hiroshima J. Med. Sci.* 24, 185–193.
- Teixeira, R.D., Ribeiro, H.A., Gomes, M.T., Lopes, M.T., Salas, C.E., 2008. The proteolytic activities in latex from *Carica candamarcensis*. *Plant Physiol. Biochem.* 46, 956–961.
- Toon, S., 1996. The relevance of pharmacokinetics in the development of biotechnology products. *Eur. J. Drug Metab. Pharmacokinet* 21, 93–103.
- USP 24, 2000. *The National Formulary – NF 19*. United States Pharmacopeia Convention, Rockville.
- USP 34, 2011. *The National Formulary – NF 29*. United States Pharmacopeia Convention, Rockville.
- Wald, M., 2008. Exogenous proteases confer a significant chemopreventive effect in experimental tumor models. *Integr. Cancer Ther.* 7, 295–310.
- Wasan, K.M., 2002. The role of lymphatic transport in enhancing oral protein and peptide drug delivery. *Drug Dev. Ind. Pharm.* 28, 1047–1058.